

The effect of oxygen lancing into a furnace alloy tap-hole: A computational case study for an open-bath furnace

M.W. Erwee^{1,2*}, Q.G. Reynolds^{3,4} and J.H. Zietsman^{1,5}

¹Department of Material Science and Metallurgical Engineering, University of Pretoria, Pretoria, 0002, South Africa

²SamancorCr, Johannesburg, 2196, South Africa, *Corresponding author: markus.erwee@gmail.com;

³Pyrometallurgy Division, Mintek, 200 Malibongwe Dr, Randburg, Gauteng, 2194, South Africa

⁴Department of Process Engineering, Stellenbosch University, Stellenbosch. 7602, South Africa

⁵Ex Mente Technologies, Pretoria, 0002, South Africa

ABSTRACT

The opening of a furnace tap-hole with an oxygen lance is a complex phenomenon that is not well understood in a quantitative way. By means of a case study, the effect of lancing on flow in and around the tap-hole area at the hot face and potential chemical wear of the refractory material are studied with multiphase fluid flow and thermochemistry models. By decoupling the modelling work into two separate sections, it is possible to obtain more quantitative results on the effect of lancing into process material such as alloy.

INTRODUCTION

The opening of tap-holes by oxygen lancing has been in practice for a long time. It is claimed that the invention of the oxygen lance pipe, specifically for tap-hole opening was done by Dr Ernst Menne in 1901 and that the practice of lancing was the primary means of tap-hole opening until the late 1960s [1]. The basic principle of opening a furnace tap-hole using an oxygen lance is simple: oxidation of the metallic lance, usually iron-based, causes intense heat at the tip of the lance, melting away tap-hole clay in the tap-hole, facilitating the flow of molten material from the furnace.

Flowrates of oxygen through long, thin lances (ca. 10-30 mm in diameter) are in the region of 110-600 Nm³/h depending on the application involved, with tip temperatures on burning quoted to be well in excess of 2000K [2, 3].

Oxygen used in the lancing process is not fully consumed, with some 50-60% by volume bypassing the lance tip. This excess oxygen interacts with both the tap-hole itself as well as process material inside the furnace. Oxidation of especially carbon-based tap-hole refractories is well known as a contributing mechanism of wear and damage to the tap-hole assembly [2, 21].

1. PURPOSE AND SCOPE OF THIS WORK

The scope of this paper is about lancing into the alloy tap-hole of an open-bath ferrochrome furnace with a partially worn tap-block, and with a layer of slag present on top of the alloy bath.

Despite drilling as primary means of tap-hole clay removal, lancing remains essential in many processes to complete tap-hole opening. Partially frozen process material blocking or constricting the flow of material from the furnace [4] could necessitate excessive lancing to minimize tapping time. In turn, the extent to which excess oxygen interacts with process material in and around the tap-hole area inside the furnace increases. In this work, the potential effects of lancing into process material was studied by means of modelling. In this paper, a very particular case study is used to illustrate how one could approach the problem by combining multiphase fluid flow modelling and basic thermochemical calculations.

Two questions were to be answered:

- To what degree does oxygen flow alone contribute to flow around the tap-hole entrance into the furnace?
- How does alloy oxidation by excess oxygen affect the tap-hole assembly, if at all?

Integrating thermochemistry and reaction kinetics into a multiphase flow model was beyond the scope of this project, because of the computational cost for such a large-scale simulation. However, as will be shown, practical answers can emerge from studying the problem in a decoupled manner.

2. COMPUTATIONAL MULTIPHASE FLUID FLOW MODEL

The volume of fluid method was used to approach the multiphase fluid flow component of the study [5]. The governing equations and boundary conditions for this flow problem is described in previous work [6].

2.1. System description and computational domain

A 1/6th slice of a 12 m diameter open-bath furnace was chosen as the computational domain. The choice of the slice size was considered reasonable to study flow around the tap-hole area, while limiting computational cost. This simplification was found to be acceptable since initial simulation results showed that flow in the radial and axial direction did not extend very far at all. A tap-block of 0.4 m in height and width protruding 0.1 m into the bottom half of the furnace was further assumed based on typical dimensions of industrial furnaces in which the tap-hole region has worn away to some extent. The tip of the 0.25 m diameter lance extended 2.5 cm into the alloy bath. The computational domain is shown in figure 1.

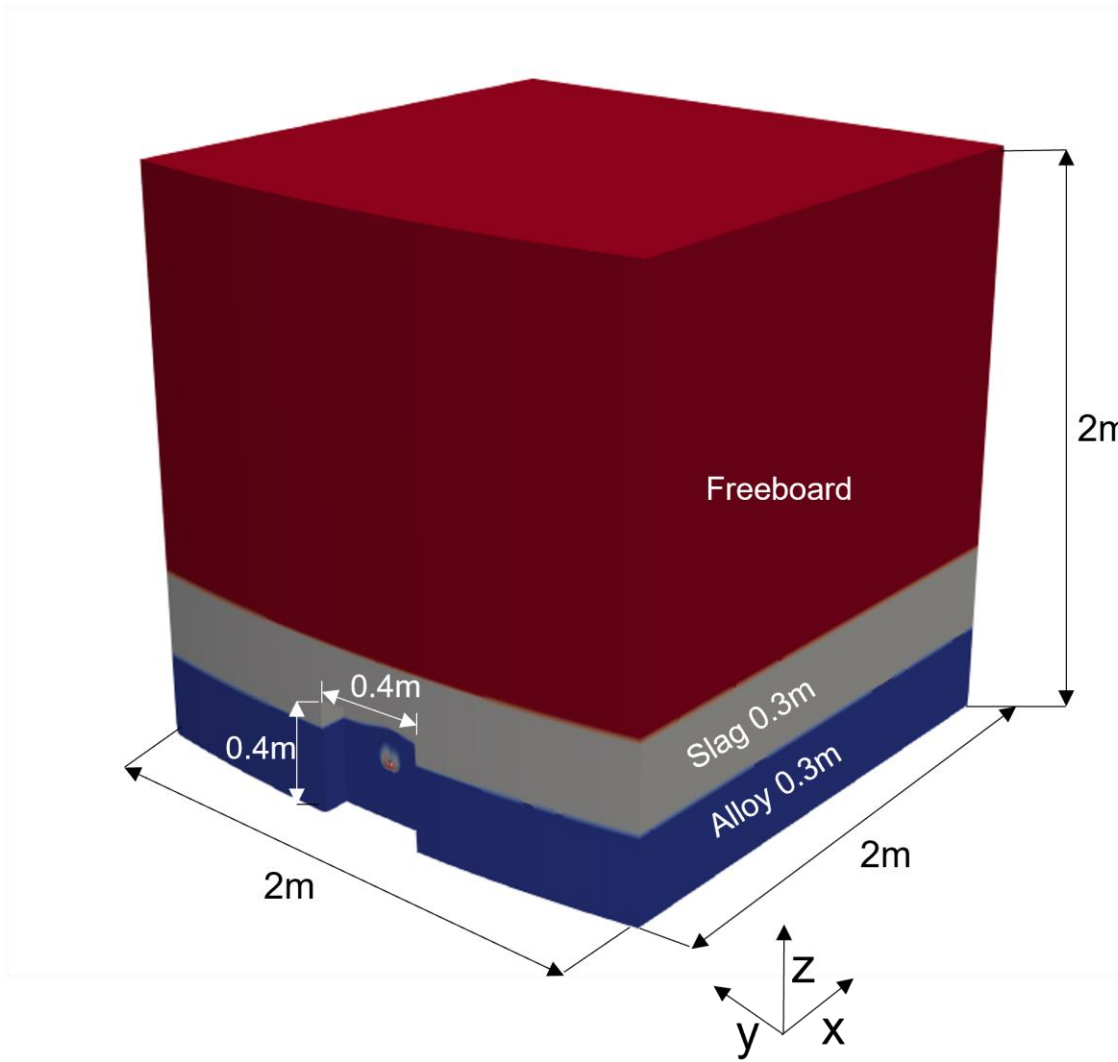


Figure 1: 3D computational domain. Blue: alloy bath, grey: slag bath, red: freeboard. Note that the geometry is a 1/6th slice of a 12 m diameter furnace, the electrode is 6 m in the radial direction from the outer edge of this geometry. The indented section of 0.4 x 0.4 m is 0.1 m deep and represents the outline of the tap-block geometry, not the physical block itself. The center of the tap-hole is 0.20 m above the bottom of the alloy bath.

2.2. Model inputs

The alloy and slag compositions were taken from work related to DC ferrochrome smelting done at Mintek [7], and are shown in Table 1. Based on these compositions, approximations were made for alloy and slag density as well as viscosity at temperatures of 1550°C for the alloy and 1850°C for the slag. These temperatures are above the liquidus temperatures of both alloy (1529°C) and slag (1836°C) as calculated in FactSage 8.0.

Table 1: Composition of the alloy and slag used in material property calculations (mass %).

Cr	Fe	C	Si	Comment
51.5	38.2	8.8	1.5	Alloy, taken from reference [7] and normalized to 100 mass %.
<hr/>				
MgO	Al₂O₃	SiO₂	CaO	
18.0	42.3	23.3	16.4	Slag, from reference [7], normalized to four components to exclude small portion of undissolved chromite. (In DC open-bath smelting, the amount of undissolved chromite is usually very small).

The alloy density was estimated to be 6600 kg/m³, and the slag density 2780 kg/m³. Both values were estimated using the molar volume approach. Data for alloy density calculations were taken from Jimbo and Cramb [8] as well as Battezzati and Greer [9] and data for the molar volume of the slag were taken from Mills [10]. Alloy viscosity was taken from Kawai [11] to be ca. 0.005 Pa.s and slag viscosity was estimated as 0.04 Pa.s with the viscosity model in FactSage 8.0 (melts database).

Slag surface tension was calculated using the method described by Hanao [12], whilst an estimate for the alloy was estimated using data from Keene [13] and Kawai [14]. The interfacial tension values for the gas-slag, gas-alloy and alloy-slag interfaces were determined as 0.45, 0.1, and 0.12 respectively.

The alloy bath depth was assumed to be 0.3 m measured from the bottom of the furnace hearth, and the slag bath depth 0.3 m extending from the top of the alloy bath. The linear velocity of pure oxygen gas used for simulations was taken to be 20 m/s and specified as an inlet boundary condition at the lance tip. This velocity was calculated by dividing an average recommended flowrate for a typical lance divided by the cross sectional area of the lance and assuming that the oxygen bypass is ca. 67% [2].

2.3. Modeling framework and solver used

The standard *multiphaseInterFoam* [22] solver in the open-source framework OpenFOAM® v2112 [15] was used for flow simulations.

In OpenFOAM® the Navier-Stokes, continuity, and phase conservation equations governing the different fields are discretized using the finite-volume method. The volume-of-fluid (VOF) method was used to account for phase separation [5].

In this particular set of work, the interest was on studying the large scale flow behavior and not the detailed microscale flows around the tip of the lance, hence turbulence models were turned off for this study. In future work, models where turbulence is accounted for is planned.

Essentially, three equations are solved for the problem, first the equation for the conservation of momentum:

$$\frac{\partial(\rho\mathbf{u})}{dt} + \nabla \cdot (\rho\mathbf{u}\mathbf{u}) + \nabla P = \nabla \cdot \tau_{ij} - \left[\gamma \nabla \cdot \left(\frac{\nabla \alpha}{|\nabla \alpha|} \right) \right] \nabla \alpha + \rho \mathbf{g} \quad [\text{Eq 1}]$$

where ρ is density, \mathbf{u} the velocity, P pressure, τ_{ij} the viscous shear force term, and γ is surface tension (all physical properties are interpolated linearly in the models). The α term is the phase fraction for each phase (gas, slag and alloy in this case).

The further equations solved are for mass conservation:

$$\frac{\partial \rho}{dt} + \nabla \cdot (\rho \mathbf{u}) = 0 \quad [\text{Eq 2}]$$

$$\frac{\partial \alpha}{dt} + \nabla \cdot (\alpha \mathbf{u}) = 0 \quad [\text{Eq 3}]$$

The velocity and pressure fields at each time step was calculated using the Pressure Implicit with Splitting of Operators predictor-corrector (PISO) algorithm. Gradient-limited discretizations were used for the divergence terms, except for those related to the phase fraction field, for which the Multidimensional Universal Limiter for Explicit Solution (MULES) limiter was used to perform interface compression and capturing.

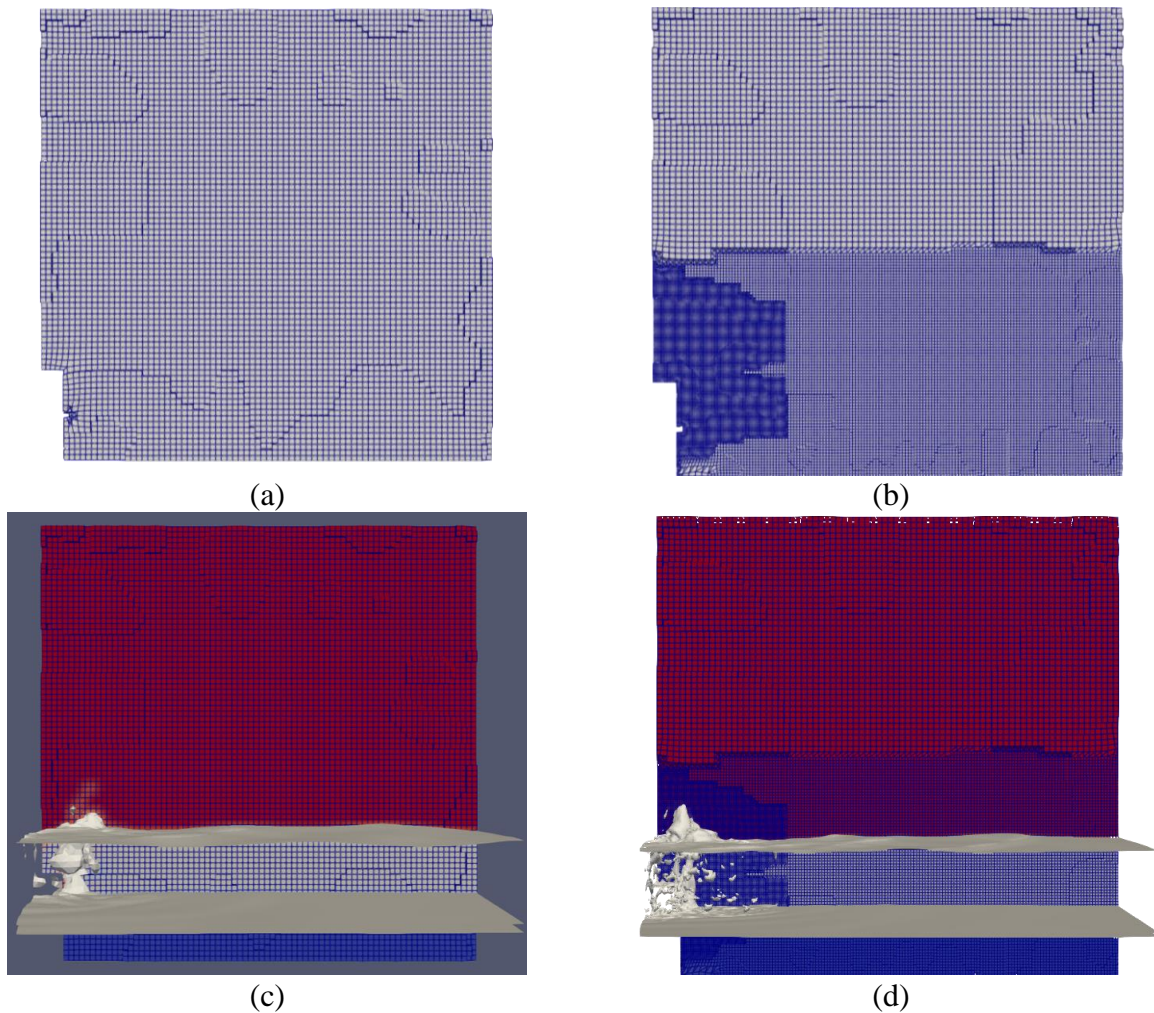
To ensure numerical stability, a Courant number of 0.5 or below was maintained with adaptive time-stepping.

Simulations were performed on a Linux-based supercomputing cluster using 640 CPU cores to simulate 5 seconds of real-time. Simulations took approximately 70 hours to solve the large scale meshes. A typical compute node on the cluster used consists of a 24 core Intel Xenon CPU (2.6GHz) with 128GB RAM, but the problem scaled best to using 40 nodes x 16 cores each.

2.4. Step-wise meshing approach of the computational domain

Meshing was done with cfMesh [16]. The scale at which these simulations need to be done implies a significant use of computing resources. To resolve flow, a very fine mesh was required. Since the degree of interaction around the tap-hole is not known beforehand, simulations were first done on a coarse mesh. The iso-surfaces (approximate threshold for the slag-alloy and slag-gas interfaces) for the alloy and slag were extracted at several time steps and used to refine the mesh locally. This approach has been proven quite effective in previous work of similar scale [17]. An example section through the middle of the computational domain reveals an initial coarse mesh, e.g. see Figure 2 (a).

The coarse mesh typically consisted of 500,000 elements. After 5 seconds in real time, the result for the calculation at low resolution is visible in Figure 2 (c). Note that this view includes the iso-surfaces of the alloy (lower grey surface) and slag (higher grey surface). A view looking into the tap-hole itself is shown in Figure 2 (e). A final high resolution mesh is shown in Figure 2 (b), (d) and (f) – these meshes contained roughly 3.2 million elements.



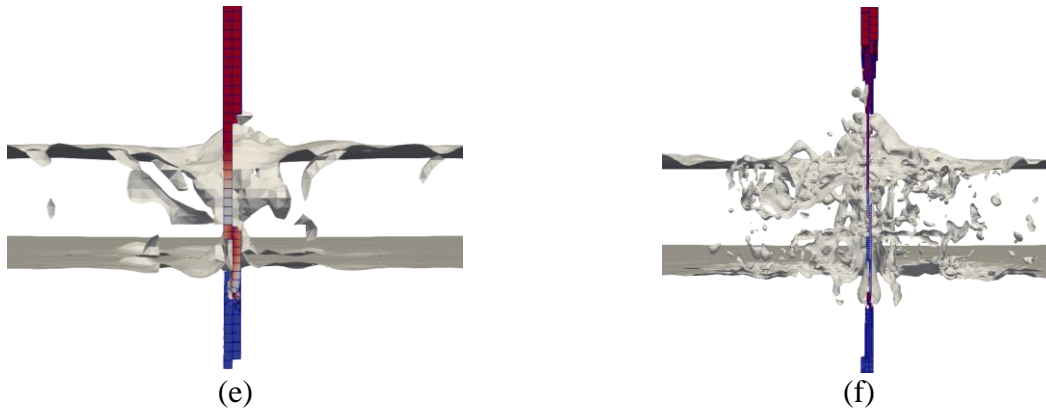


Figure 2: Meshing strategy. Figures on the left are for the low-resolution case, while figures on the right are high resolution cases (at timestep of 5 s).

2.5. Summary of the computational results

A convenient side-effect of the meshing strategy is that it yields an indication of the volume to which most of the oxygen gas flow is constrained over time.

With the low gas density ($\sim 1.29 \text{ kg/m}^3$) compared to that of the alloy (6600 kg/m^3), it is not surprising that once the gas enters the melt it almost immediately flows upwards through the alloy-slag interface. Because of the proximity of the lance tip to the tap-block, gas moves up against the tap-block and furnace wall. Although this occurs for a short time, successive attempts at lancing could add to this effect over time.

The calculated flow patterns confirm what is qualitatively expected, based on alloy and gas material properties. In addition, the computational results provide a more quantitative basis for assessing heat and mass transfer in the tap-hole area, and to inform laboratory testing, e.g. rotary finger refractory testing, to get a better understanding of how much the effects of lancing could contribute to overall refractory wear.

Chemical interaction between refractory materials and slag or alloy in furnaces is inevitable especially where temperatures are elevated significantly beyond normal furnace operating temperatures. At the same time, thermal shock and subsequent spalling of refractory materials are quite common wear mechanisms where sudden temperature changes occur.

Oxygen lancing into furnace tap-holes, especially in contact with oxidizable alloy, has the potential to contribute to both the aforementioned wear mechanisms, although in short bursts at a time. One could consider this being the equivalent of ‘death by a thousand cuts’ for a furnace tap-block. Tap-floor staff could easily spend significant time to open tap-holes if there is pressure to drain a furnace, and this is a common occurrence in several industrial processes.

The magnitude of velocity from the middle of the lance tip in each direction is plotted in figure 3.

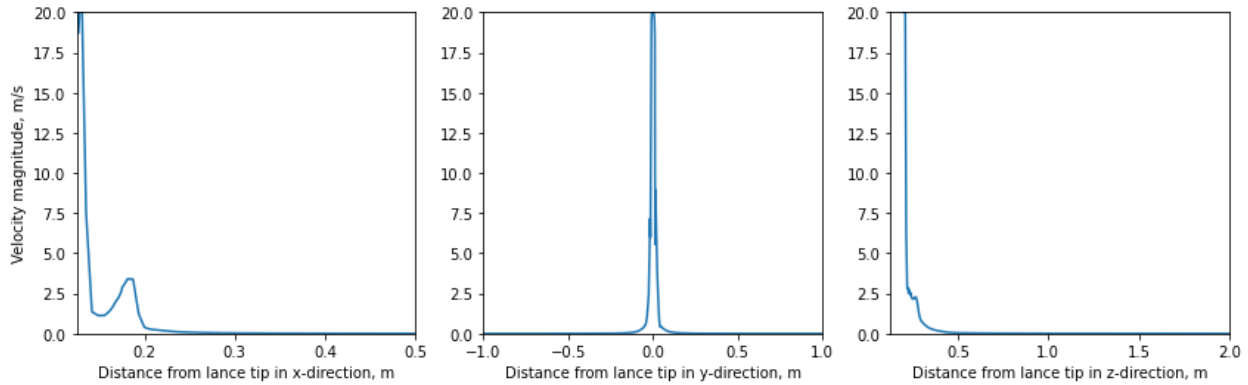


Figure 3: Velocity magnitude profiles from the lance tip in each of the x (radially into the bath), y (tangential) and z (axial) directions ($t=0.1s$). See figure 1 for coordinate system. The middle of the lance is the origin of each plot.

From the results it is quite clear that the low density gas, as expected collects as bubbles flowing upwards into the slag bath, with very little flow towards the sides (tangential, y-direction) and into the bath (radial, x-direction).

The results from the computational model gives an indication of the ‘interaction’ volume of the gas plume with the alloy phase. Using the interaction volume, a few calculations can be made to estimate the propensity for chemical wear and, for example, thermal behavior in and around the tap-hole area due to lancing; this is covered in the next section. In this set of results, it is evident that most of the flow (highest velocities) is concentrated in an area directly around the tip of the lance. From the results, it was calculated that the immediate interaction volume was 1.5 liters – a small region, but an area where mass and heat transfer would be extremely high for moments when the lance enters the melt and oxygen is injected. If the entire fine refined area (dark blue section in Figure 2 (d) is taken as the interaction volume), the figure is roughly 100 times the immediate interaction volume. For thermochemical calculations the volumes considered were the immediate volume and double the immediate volume, to make more conservative calculations as well.

3. THERMOCHEMICAL CALCULATIONS

Thermochemical calculations were done using data from FactSage 8.1, implemented with ChemApp for Python [18]. Solution models from the SGTE solution database were used for describing alloy phases, while oxides and oxide solutions originating from alloy oxidation were taken described with phases and pure compounds of the FTOxid database. FactPS pure substance data were used for the gas phase.

Based on the typical volumetric flow of gas that bypasses into the melt, an adiabatic calculation was made for a total of 2 minutes of total blowing time. Although kinetic effects could impede the reaction rate, the overall effect on temperature should still be accurate given the fact that the flow simulations show significant mixing in the interaction volume with fresh alloy readily moving into the region.

From the thermochemical calculation, the predicted reaction product was CO gas, which is expected at these high temperatures and with the abundance of carbon in the alloy bath. Oxidation of carbon in the alloy bath is highly exothermic.

The result of the adiabatic calculation is shown in Figure 4. Effectively, what is shown is the maximum temperature that the interaction volume could reach after a certain amount of oxygen has reacted with alloy for the immediate interaction volume calculated in the computational flow model as well as an interaction volume double in size to make a conservative estimate of the temperature increase.

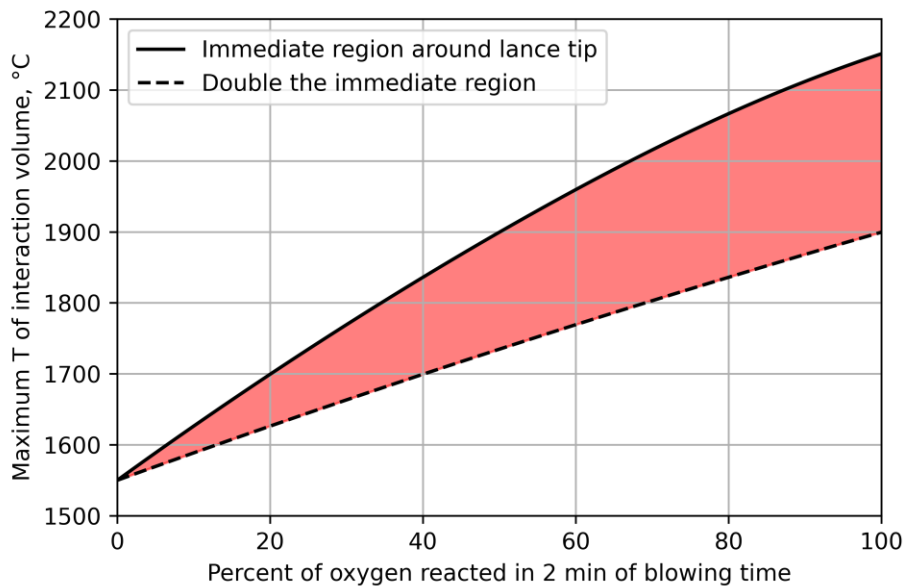


Figure 4: Estimated adiabatic temperature of the alloy-gas interaction volume

It is quite interesting to see that for a small time spent in the alloy bath, a lance injecting oxygen into the melt can temporarily increase the temperature in the immediate vicinity of the tap-block by a significant margin. Temperature maxima for each instance are between 1900 and 2150°C compared to the average alloy bath temperature of 1550°C. These sudden bursts of energy and temperature spikes on the hot face of the tap-block refractories can lead to increased wear due to spalling, over and above wear from material flow through the tap-block. Realistically, the temperature reach would be somewhere in the read shaded area, rather than the absolute maxima shown due to energy dissipation into the bath.

Aside from the possibility of spalling, the propensity for chemical wear of the tap-hole area does increase with increasing temperature. This is true for almost all refractories, with near exponential increases in wear once a certain precipice is breached (example, see refs [19, 20]).

To test the idea, two refractory materials for tap-blocks were chosen as basis for chemical interaction calculations with the alloy at different temperatures. The two materials chosen were carbon and alumina chrome. To simplify the problem, it was assumed that 100g of the refractory was in contact with 100g of the alloy – in reality, fresh alloy should reach the tap-block easily because of mixing due to lancing.

The results of the calculations are shown in Figure 5. In both cases, there is some wear expected at extreme temperatures predicted using the adiabatic calculation.

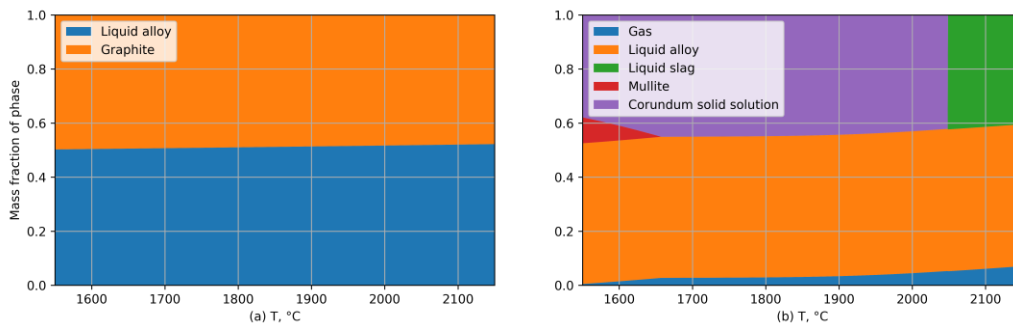


Figure 5: Phase chemistry of 100g alloy phase in contact with 100g refractory: (a) carbon-based block, (b) $\text{Al}_2\text{O}_3\text{-Cr}_2\text{O}_3$ block.

Although the wear contribution seems small, there is scope to adjust the strategy of lancing, especially when tap-blocks are somewhat worn. In the case of the carbon-based block, a small amount of refractory dissolves to saturate the melt in carbon (see figure 5 (a)).

In the case of the $\text{Al}_2\text{O}_3\text{-Cr}_2\text{O}_3$ block ('corundum solid solution+mullite' phase in figure 5 (b)), reaction of carbon with Cr_2O_3 in the refractory is possible if the refractory is fully wettable by the alloy, this is also the source of the small amount of gas shown in the figure. At temperatures above 2050°C, the brick would melt under these conditions, hence the appearance of the liquid slag phase.

4. CONCLUSIONS

The effect of lancing into pyrometallurgical furnace tap-holes was studied using a decoupled approach, i.e. using a fluid flow model to quantify an interaction volume between oxygen gas from the lance and the molten alloy in the furnace and then using the result to inform a set of thermochemical calculations.

While a fully coupled multiphase fluid flow – thermochemistry model seems like a wonderful idea, practical answers can emanate from studying the problem in a decoupled way at much less computational cost. Such hybrid modelling can be used not only to inform operations, but also inform more sophisticated laboratory experiments by doing a-priori computational studies on the industrial scale problem.

In this work, the immediate interaction volume between excess oxygen flowing from the lance tip and the alloy bath close to the tap-block is concentrated in a volume of approximately 1.5 litres for typical flowrates of oxygen. Heat released from reaction between the alloy and oxygen is sufficient to increase the temperature in this region by as much as 400°C, which dramatically increases the propensity for refractory wear.

5. ACKNOWLEDGEMENTS

The authors would also like to thank the Centre for High Performance Computing (Cape Town) for making resources available for this project. This paper is published by permission of Mintek. Support from SCr for this paper is greatly appreciated.

On behalf of all authors, the corresponding author states that there is no conflict of interest.

6. REFERENCES

- [1] A. Dienenthal, “A short history of the development of tapping equipment,” Paper presented at the 2014 Furnace Tapping Conference, Muldersdrift, South Africa, May 2014, vol. 1, pp. 203–216. <https://www.saimm.co.za/Conferences/FurnaceTapping/203-Dienenthal.pdf>, Accessed: 4 October 2021
- [2] D. Morales, C. Morales, and S. Nunes, “Tap-hole opening: advances and improvements,” Paper presented at the 2018 Furnace Tapping Conference, Kruger National Park, South Africa, Oct. 2018, pp. 231–250. <http://www.saimm.co.za/Conferences/FurnaceTapping2018/231-Morales.pdf>, Accessed: 2 April 2022.
- [3] T. Martí-Rosselló, P. Ray, J. Li, and L. Lue, *Ind. Eng. Chem. Res.*, vol. 60, no. 21, pp. 7788–7801, Jun. 2021, <https://doi.org/10.1021/acs.iecr.1c00532>
- [4] S. G. Mgenge and J. D. Steenkamp, “Furnace tapping practice at Tronox Namakwa Sands,” Paper presented at the 2014 Furnace Tapping Conference, Muldersdrift, South Africa, May 2014, pp. 137–146. <https://www.saimm.co.za/Conferences/FurnaceTapping/137-Mgenge.pdf>

- [5] C. W. Hirt and B. D. Nichols, *J. Comput. Phys.*, vol. 39, no. 1, pp. 201–225, Jan. 1981, [https://doi.org/10.1016/0021-9991\(81\)90145-5](https://doi.org/10.1016/0021-9991(81)90145-5)
- [6] M. W. Erwee, Q. G. Reynolds, and J. H. Zietsman, *JOM*, vol. 68, no. 6, pp. 1556–1562, Jun. 2016, <https://doi.org/10.1007/s11837-016-1873-6>
- [7] I. J. Geldenhuys, “Aspects of DC chromite smelting at Mintek – An overview,” Paper presented at The Thirteenth International Ferrous Alloys Congress, Almaty, Kazakhstan, Jun. 2013, pp. 31–47. <https://www.pyrometallurgy.co.za/InfaconXIII/0031-Geldenhuys.pdf> Accessed: 2 April 2022.
- [8] I. Jimbo and A. W. Cramb, *Metall. Trans. B*, vol. 24, no. 1, pp. 5–10, Feb. 1993, <https://doi.org/10.1007/BF02657866>
- [9] L. Battezzati and A. L. Greer, *Acta Metall.*, vol. 37, no. 7, pp. 1791–1802, Jul. 1989, [https://doi.org/10.1016/0001-6160\(89\)90064-3](https://doi.org/10.1016/0001-6160(89)90064-3)
- [10] K. C. Mills, M. Hayashi, L. Wang, and T. Watanabe, “The Structure and Properties of Silicate Slags,” in *Treatise on Process Metallurgy*, Elsevier, 2014, pp. 149–286. <https://doi.org/10.1016/B978-0-08-096986-2.00008-4>
- [11] Y. Kawai, M. Tsuji, and M. Kanemoto, *Tetsu--Hagane*, vol. 60, no. 1, pp. 38–44, 1974, https://doi.org/10.2355/tetsutohagane1955.60.1_38
- [12] M. Hanao, T. Tanaka, M. Kawamoto, and K. Takatani, *ISIJ Int.*, vol. 47, no. 7, pp. 935–939, 2007, <https://doi.org/10.2355/isijinternational.47.935>
- [13] B. J. Keene, *Int. Mater. Rev.*, vol. 38, no. 4, pp. 157–192, Jan. 1993, <https://doi.org/10.1179/imr.1993.38.4.157>
- [14] Y. Kawai, K. Mori, M. Kishimoto, K. Ishikura, and T. Shimada, *Tetsu--Hagane*, vol. 60, no. 1, pp. 29–37, 1974, https://doi.org/10.2355/tetsutohagane1955.60.1_29
- [15] *OpenFOAM*. 2022. <https://www.openfoam.com/>, Accessed 2 April 2022.
- [16] *cfMesh*. 2022. <https://cfmesh.com/>, Accessed 6 January 2022.
- [17] Q. G. Reynolds and J. E. Olsen, “Modelling of Metal Loss in Ferromanganese Furnace Tapping Operations,” in *Materials Processing Fundamentals 2021*, J. Lee, S. Wagstaff, A. Anderson, F. Tesfaye, G. Lambotte, and A. Allanore, Eds. Cham: Springer International Publishing, 2021, pp. 83–92. https://doi.org/10.1007/978-3-030-65253-1_7
- [18] *ChemAppPy (ChemApp for Python)*. <https://gtt-technologies.de/chemapp-for-python/>, Accessed 14 July 2022/
- [19] J. D. Steenkamp, *J. South. Afr. Inst. Min. Metall.*, vol. 119, no. 6, 2019, <https://doi.org/10.17159/2411-9717/669/2019>
- [20] M. B. Sitefane and J. D. Steenkamp, “The Evaluation of Chemical Wear of Carbon-Based Tap-Hole Refractories in Ferrochrome Production,” Paper presented at the 2022 Furnace Tapping Conference, pp. 297–309. https://doi.org/10.1007/978-3-030-92544-4_22
- [21] P. O’Shaughnessy, H. van der Merwe, and S. Botes, “Tap-hole repair: the UCAR®V Repair Solution”. Paper presented at the 2014 Furnace Tapping Conference, Muldersdrift, South Africa, May 2014, vol. 1, pp. 79–86. <https://www.saimm.co.za/Conferences/FurnaceTapping/079-O'Shaughnessy.pdf>, Accessed 21 September 2022.
- [22] P. Andersson, “Tutorial multiphaseInterFoam”, Chalmers University, 2010, Online reference accessed 21 September 2022. http://www.tfd.chalmers.se/~hani/kurser/OS_CFD_2010/patrikAndersson/patrikAnderssonReport.pdf